

Beam-based characterization of plasma density in a capillary-discharge waveguide

EP

Cite as: AIP Advances **11**, 065217 (2021); <https://doi.org/10.1063/5.0051423>
Submitted: 30 March 2021 • Accepted: 25 May 2021 • Published Online: 10 June 2021

 S. Romeo, M. Cesarini, A. Del Dotto, et al.

COLLECTIONS

 This paper was selected as an Editor's Pick



View Online



Export Citation



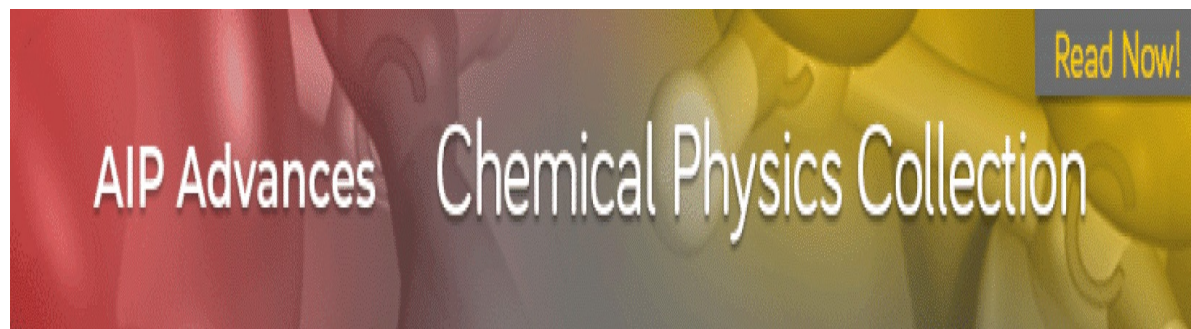
CrossMark

ARTICLES YOU MAY BE INTERESTED IN

[Laser-heated capillary discharge plasma waveguides for electron acceleration to 8 GeV](#)
Physics of Plasmas **27**, 053102 (2020); <https://doi.org/10.1063/5.0002769>

[Perspectives on the generation of electron beams from plasma-based accelerators and their near and long term applications](#)
Physics of Plasmas **27**, 070602 (2020); <https://doi.org/10.1063/5.0004039>

[Combining laser interferometry and plasma spectroscopy for spatially resolved high-sensitivity plasma density measurements in discharge capillaries](#)
Review of Scientific Instruments **92**, 013505 (2021); <https://doi.org/10.1063/5.0021117>



Beam-based characterization of plasma density in a capillary-discharge waveguide

Cite as: AIP Advances 11, 065217 (2021); doi: 10.1063/5.0051423

Submitted: 30 March 2021 • Accepted: 25 May 2021 •

Published Online: 10 June 2021



View Online



Export Citation



CrossMark

S. Romeo,^{1,a)}  M. Cesarini,^{1,2} A. Del Dotto,¹ M. Ferrario,¹ M. Galletti,¹  R. Pompili,¹  and V. Shpakov¹

AFFILIATIONS

¹Laboratori Nazionali di Frascati, Via Enrico Fermi 40, 00044 Frascati (Rome), Italy

²University of Rome "Sapienza", Piazzale Aldo Moro 5, 00185 Rome, Italy

^{a)} Author to whom correspondence should be addressed: stefano.romeo@lnf.infn.it

ABSTRACT

Next-generation plasma-based accelerators can push electron bunches to gigaelectronvolt energies within centimeter distances. In these devices, the accelerating force is provided by a driver pulse, either a laser pulse or a particle bunch, that loses its energy into the plasma generating huge electric fields up to tens of GV/m. The stability of such fields strongly depends on plasma density, whose exact value should be precisely known and controlled. However, currently available methods based on spectroscopic or interferometric techniques find it very difficult to measure plasma density lower than $10^{15-16} \text{ cm}^{-3}$ in capillary-discharge waveguides. Here, we present a novel diagnostic tool that allows us to estimate the average density of a plasma capillary by probing it with an ultra-relativistic electron beam. The plasma density and the generated accelerating field are inferred by analyzing the beam longitudinal phase space after its interaction with the plasma. The results are validated by simulations showing excellent agreement.

© 2021 Author(s). All article content, except where otherwise noted, is licensed under a Creative Commons Attribution (CC BY) license (<http://creativecommons.org/licenses/by/4.0/>). <https://doi.org/10.1063/5.0051423>

Plasma-based devices have been proven to be a valid candidate for the development of a new generation of accelerating machines.¹ Experimental results have shown the possibility to achieve huge accelerating gradients, up to tens of GV/m,²⁻⁴ while preserving the energy spread of the accelerated beams.⁵ In addition to this, plasma structures have been successfully implemented also as active lenses^{6,7} and dechirpers.⁸⁻¹⁰

A high degree of control of the plasma density is mandatory for the correct operation of such devices. Several methods have been developed in order to measure the plasma density with high sensitivity ($\Delta n_p \approx 10^{13} \text{ cm}^{-3}$).¹¹⁻¹⁴ For the discharge capillary setup, the best results are guaranteed by Stark broadening^{15,16} and interferometric techniques,^{17,18} but nowadays their sensitivity is limited to $1.8 \cdot 10^{15} \text{ cm}^{-3}$. The idea to use a probe beam to characterize the plasma density has been devised as well. With a given plasma profile, the longitudinal profile of a charged particle beam was retrieved from the measurement of the time-resolved energy variation due to wakefield effects.¹⁹ Another work pointed out that it is possible to retrieve the plasma density by analyzing the beam longitudinal phase space (LPS) or its transverse profile through Fourier analysis.²⁰ However, as pointed out by the authors, the interpretation of the results is not straightforward due to the overlap of different

modes in the Fourier spectra that could require additional numerical simulations. In this work, we present an innovative method to retrieve the value of the plasma density based on the analysis of the beam LPS after its interaction with the plasma that provides a well-defined value for the plasma density and relative uncertainty. We analyze the slice energy of the probe beam, both with and without the interaction with the plasma, thus retrieving the time-resolved deformation of the LPS and the longitudinal field $E_z(\xi)$ generated in the beam-plasma interaction. A fit of the latter is performed, following the plasma equations in the cold fluid approach,²¹⁻²³ to retrieve the plasma skin depth $k_p = (e^2 n_p / \epsilon_0 m_e c^2)^{1/2}$, where n_p is the plasma density, e is the electron charge, ϵ_0 is the permittivity of vacuum, m_e is the electron mass, and c is the speed of light. A comparison is made by carrying out numerical simulations. Such a comparison has shown a good agreement between the measured and simulated LPSs and, in turn, a high degree of reliability of the retrieval method.

The experiment was carried out at the SPARC_LAB test facility^{24,25} in the framework of the *EuPRAXIA@SPARC_LAB* project.²⁶⁻²⁸ The experimental setup is shown in Fig. 1. The beam is produced by the SPARC photo-injector, consisting of an RF gun, followed by three accelerating sections. The experimental chamber includes a triplet of permanent magnet quadrupoles for injection

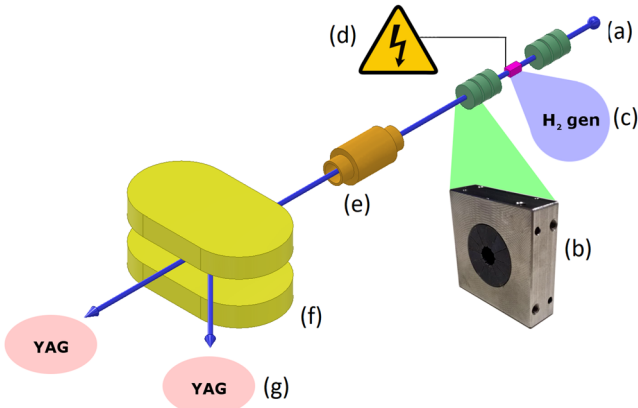


FIG. 1. The beam (a) is produced by means of the SPARC photo-injector. The experimental chamber includes an injection extraction system consisting of two triplets of permanent magnet quadrupoles (b) and the plasma module. The plasma is generated inside a 3 cm long capillary with a radius $r_C = 0.5$ mm that is filled with hydrogen gas by an hydrogen generator (c). The plasma is produced by applying a high voltage to the two electrodes placed at the two ends of the capillary (d). The diagnostic system consists of an RF-deflector (e) coupled to a dipole spectrometer (f) in order to display the LPS of the bunch on screens (g).

into the plasma capillary and another for the extraction of the beam downstream. The plasma is generated inside a 3 cm long capillary with a radius $r_C = 500$ μm that is hydrogen-filled. The plasma is produced by ionizing the hydrogen gas through a high-voltage discharge applied at the two electrodes located at the capillary extremities. The diagnostic system consists of an RF-deflector²⁹ and a magnetic spectrometer that allow us to measure the beam LPS in correspondence with a scintillating YAG screen installed on a 14° dogleg beamline. A second screen is installed on a straight line in order to measure the beam emittance through the quadrupole scan technique.³⁰

The plasma density inside the capillary reaches its peak value during the discharge, and afterward, it begins to decrease over time due to the recombination of plasma ions and electrons. By varying the delay between the time of arrival of the electron bunch and the beginning of the discharge, one can control the plasma density experienced by the electron bunch inside the capillary. Namely, this allows us to use the beam as a probe to measure the evolution of the plasma density over time. This setup allowed us to perform a scan for investigating the variation of the bunch LPS after the interaction with the plasma at different delays. One can extract the energy variation over the longitudinal coordinate of the bunch $\Delta\mathcal{E}(\xi)$ and thus the longitudinal electric field $E_z(\xi) = \Delta\mathcal{E}(\xi)/\ell$, given the fixed length of the plasma profile ℓ .

In order to describe the behavior of the longitudinal field, we recall the well-known solutions in the linear regime for the cold plasma model in the fluid approach. This approximation^{21–23} holds for low density bunches $\eta = n_b/n_p \ll 1$, where n_b is the bunch density, or for high density bunches with a low normalized charge $\bar{Q} = N_b k_p^3/n_p$, where N_b is the number of bunch electrons.³¹ The longitudinal field can be derived as

$$E_z(r, \xi) = R(r)Z'(\xi), \quad (1)$$

where $R(r)$ and $Z(\xi)$ are the transverse and longitudinal plasma response functions, respectively. By definition,

$$R(r) = k_p^2 K_0(k_p r) \int_0^r r' dr' n_{b\perp}(r') I_0(k_p r') + k_p^2 I_0(k_p r) \int_r^\infty r' dr' n_{b\perp}(r') K_0(k_p r')$$

and

$$Z'(\xi) = -\frac{e}{\epsilon_0} \int_{-\infty}^{\xi} n_{b\parallel}(\xi') \cos[k_p(\xi - \xi')] d\xi'. \quad (2)$$

Assuming a weak dependence on r , $\Delta\mathcal{E}(\xi) \propto Z'(\xi)$, providing a direct link between the measurement of the LPS and the plasma skin depth k_p . With $n_{\perp}(r) = e^{-r^2/\sigma_r^2}$ and $n_{\parallel} = n_b e^{-\xi^2/2\sigma_z^2}$, we can retrieve an approximated solution for $R(0)$,²³

$$R(0) \approx k_p^2 \sigma_r^2 [0.05797 - \ln k_p \sigma_r].$$

The exact solution for $Z'(\xi)$ can be retrieved by means of a direct integration of Eq. (2),³²

$$Z'(\xi) = -\sqrt{\frac{\pi}{2}} \frac{m_e c^2}{e} \frac{n_b}{n_p} k_p^2 \sigma_z e^{-k_p^2 \sigma_z^2 / 2} \text{Re} \left[e^{ik_p \xi} (1 + \text{erf} \chi) \right], \quad (3)$$

where $\chi = \xi/\sqrt{2}\sigma_z + ik_p \sigma_z/\sqrt{2}$ and i is the imaginary unit. From Eqs. (1)–(3), the following equation is derived:

$$\Delta\mathcal{E}(\xi) = C \text{Re} \left[e^{ik_p \xi} \left(1 + \text{erf} \frac{\xi}{\sqrt{2}\sigma_z} + i \frac{k_p \sigma_z}{\sqrt{2}} \right) \right], \quad (4)$$

where C is a multiplying factor defined as

$$C = \sqrt{\frac{\pi}{2}} \frac{m_e c^2}{e} \frac{n_b}{n_p} k_p^2 \sigma_z e^{-k_p^2 \sigma_z^2 / 2} R(0) \ell. \quad (5)$$

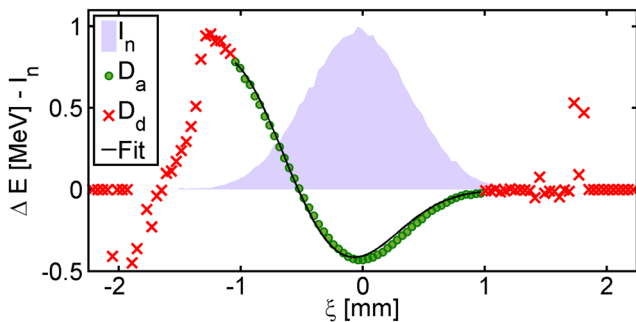
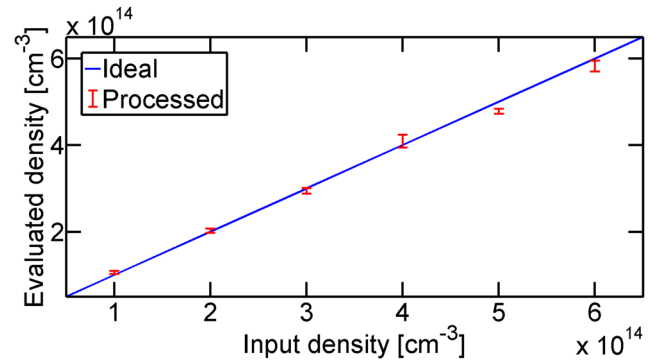
This parameter directly depends on the plasma density and bunch parameters. The beam density and normalized spot size $k_p \sigma_r$ can vary shot to shot, changing the value of C for a fixed plasma density. Since this feature could introduce further errors in the analysis, we considered it as a fit parameter, not depending on plasma density. Numerical simulations validate the reliability of our approach, providing a benchmark of the measurements performed at SPARC_LAB. We simulated the interaction of a bi-Gaussian bunch and a plasma profile with different densities ($n_p = 1-6 \cdot 10^{14}$ cm^{-3} range) by the hybrid kinetic-fluid code *Architect*. In this code, the background ions are assumed motionless and the background electrons are modeled as a 2D fluid in cylindrical symmetry. For the bunch electrons, a 3D particle in cell (PIC) model is implemented. This approach allows us to perform relatively quick simulations, directly investigating the effects on the phase space.³³ The beam at the injection is round with a transverse spot size $\sigma_{x,y} = 17$ μm . The first simulation assumes a plasma density $n_p \sim 2 \cdot 10^{14}$ cm^{-3} . The bunch parameters are set as in Table I. In order to perform a one to one comparison of the LPS simulation with the experimental measurement, we have to assume that the latter is weakly affected by the transport of the bunch downstream the plasma module, namely that the beam spot size without the RFD and spectrometer is small compared to the dispersion introduced

TABLE I. Injection bunch parameters.

Parameter	Symbol	Value
Charge	Q	200 (pC)
Energy	γ	179
Emittance	ϵ_n	1.7 (μm)
Transverse spot size	$\sigma_{x,y}$	17 (μm)
Bunch rms length	σ_z	420 (μm)
Energy spread	σ_E	0.1 (%)

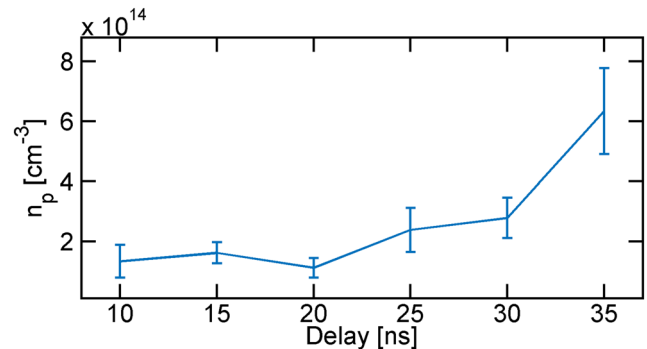
by these devices. This is a standard assumption that has been verified experimentally in our setup.³⁴ This assumption is the main limit to the rescalability of the method. In order to evaluate $\Delta\mathcal{E}(\xi)$, the time resolution of the measurement must be much lower than the plasma frequency and the energy resolution must be much lower than the energy shift introduced by the plasma. For real bunches with a finite dimension, the precision of the measurement of the LPS is limited by the bunch spot size. For our setup, this effect becomes non-negligible at low plasma densities $n_p < 10^{14} \text{ cm}^{-3}$, where the required energy resolution for accurate measurements is $\approx 10 \text{ keV}$, and at high plasma densities $n_p > 10^{17} \text{ cm}^{-3}$, where the required temporal resolution is 1–5 fs. Projecting the image on the space axis, one can retrieve the longitudinal spatial distribution of the bunch. The normalized intensity of the bunch $I_n = I(\xi)/I(\xi)_{\text{max}}$ is shown in Fig. 2. By means of a Gaussian fit, both the longitudinal position of the bunch ξ_0 and the bunch length σ_z are retrieved. The LPSs of the bunch before and after the interaction are then shifted by ξ_0 in order to be compatible with the assumptions, according to which Eqs. (1)–(3) were retrieved (the mean value of the Gaussian bunch is located at $\xi_0 = 0$). Since, in our case, the bunch is ultra-relativistic, we will consider a constant current profile, making suitable a slice approach. We will use it to retrieve the energy $\mathcal{E}(\xi)$ and the energy spread $\sigma_z(\xi)$ and to evaluate the shape of the electric field $E_z(\xi)$ by means of a Gaussian fit. The mean values of the Gaussians are then subtracted in order to obtain $\Delta\mathcal{E}(\xi)$. The slices with very low signal to noise ratios [$I_n(\xi) < 0.1$] are excluded from further analysis.

This new set of refined data is exploited in order to evaluate k_p by means of a fit based on Eq. (4), given the value for σ_z that was retrieved from the previous fit on LPS projection. The corresponding plasma density n_p was evaluated from the definition of k_p .

**FIG. 2.** Bunch normalized intensity I_n (purple area), accepted data D_a (green), discarded data D_d (red), and fit result (black) obtained by the slice analysis.**FIG. 3.** Reference line for ideal measurement output (blue). Density values retrieved from the analysis (red). The error bars are set according to the uncertainty of the fit.

Data and relative fit are plotted in Fig. 2. The same analysis was then performed for several cases in the range $n_p = 1\text{--}6 \cdot 10^{14} \text{ cm}^{-3}$. The resulting plasma densities are plotted in Fig. 3. In all the considered cases, evaluated density differs from the input density for less than 2%, proving the reliability of the retrieval method. This minor discrepancy most likely depends on the accuracy of the fit over a finite number of points, and it could be reduced by further increasing the time sampling of the bunch.

The validated method was then applied to a set of experimental measures. The LPS without the plasma was fixed to its average value over five shots. The analysis of the LPSs with the plasma has been performed separately over 20 shots per delay. For each delay, the plasma density has been evaluated as the average of the retrieved results, the error being the standard deviation of the results. The measured plasma density for different delays is plotted in Fig. 4. In Fig. 5, the most relevant phase spaces from the measurement are compared with the simulations having a corresponding plasma density. The simulations reproduce with a good degree of reliability the measured phase spaces, showing a similar shape and a comparable energy of the core. The tail of the bunch is not well reproduced. This effect is probably related to the transverse electric field generated in the closing region of the plasma bubble³⁵ that strongly defocuses the tail but not the beam core.

**FIG. 4.** Retrieved experimental plasma density at different delays.

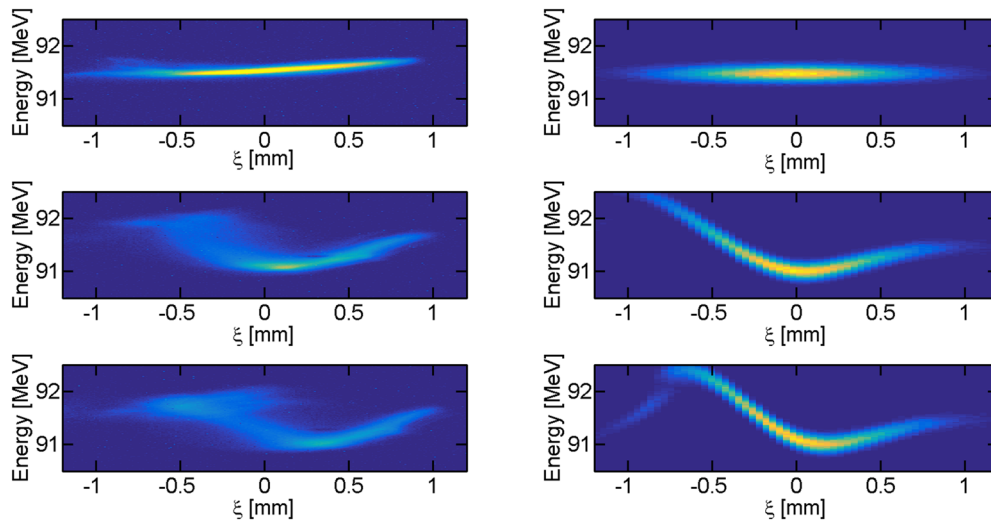


FIG. 5. Experimental LPSs (left) of the bunch with no discharge (top), with discharge delay set at 25 ns (center) and with discharge delay set at 30 ns (bottom). Numerical LPSs (right) with no plasma interaction (top), with plasma density $n_p = 3 \cdot 10^{14} \text{ cm}^{-3}$ (center), and with plasma density $n_p = 6 \cdot 10^{14} \text{ cm}^{-3}$ (bottom).

The underlying motivation for this work is the crucial need for a reliable measurement system for the plasma density inside the capillaries. Since the accelerating gradient strongly depends on the plasma density itself, future plasma-based accelerators will require a high degree of control of this parameter. We presented an innovative method that allows us to estimate the density of the plasma confined in a capillary by analyzing its interaction with an ultra-relativistic electron beam. The method is able to probe very low densities, down to $10^{14-15} \text{ cm}^{-3}$, that are usually not accessible to conventional techniques based on spectroscopic or interferometric methods. Furthermore, the method is rescalable to different density ranges and it allows us to estimate the stability of the plasma density shot-to-shot. For these reasons, we state that the presented method is highly promising for the characterization of the plasma density in capillary-discharge waveguides.

This work was partially supported by the EU Commission in the Seventh Framework Program (Grant Agreement No. 312453-EuCARD-2), the European Union Horizon 2020 research and innovation program (Grant Agreement No. 653782) (EuPRAXIA), and the INFN (Grant No. 73/PLADIP).

DATA AVAILABILITY

The data that support the findings of this study are available from the corresponding author upon reasonable request.

REFERENCES

- ¹M. J. Hogan, T. O. Raubenheimer, A. Seryi, P. Muggli, T. Katsouleas, C. Huang, W. Lu, W. An, K. A. Marsh, W. B. Mori *et al.*, "Plasma wakefield acceleration experiments at FACET," *New J. Phys.* **12**, 055030 (2010).
- ²W. P. Leemans, B. Nagler, A. J. Gonsalves, C. Tóth, K. Nakamura, C. G. R. Geddes, E. Esarey, C. B. Schroeder, and S. M. Hooker, "GeV electron beams from a centimetre-scale accelerator," *Nat. Phys.* **2**, 696–699 (2006).

- ³I. Blumenfeld *et al.*, "Energy doubling of 42 GeV electrons in a metre-scale plasma wakefield accelerator," *Nature* **445**, 741–744 (2007).
- ⁴M. Litos *et al.*, "High-efficiency acceleration of an electron beam in a plasma wakefield accelerator," *Nature* **515**, 92–95 (2014).
- ⁵R. Pompili, D. Alesini, M. Anania, M. Behtouei, M. Bellaveglia, A. Biagioni, F. Bisesto, M. Cesarini, E. Chiadroni, A. Cianchi *et al.*, "Energy spread minimization in a beam-driven plasma wakefield accelerator," *Nat. Phys.* **17**, 499 (2021).
- ⁶R. Pompili *et al.*, "Experimental characterization of active plasma lensing for electron beams," *Appl. Phys. Lett.* **110**, 104101 (2017).
- ⁷A. Marocchino *et al.*, "Experimental characterization of the effects induced by passive plasma lens on high brightness electron bunches," *Appl. Phys. Lett.* **111**, 184101 (2017).
- ⁸Y. Wu, Y. Du, J. Zhang, Z. Zhou, Z. Cheng, S. Zhou, J. Hua, C. Pai, and W. Lu, "A preliminary experimental study of energy chirp reduction by a plasma dechirper," in *Proceedings of IPAC17* (Copenhagen, 2017), pp. 1258–1260; available at <https://inspirehep.net/files/af037edfe922974aee464635947a734a>
- ⁹R. D'Arcy, S. Wesch, A. Aschikhin, S. Bohlén, C. Behrens, M. Garland, L. Goldberg, P. Gonzalez, A. Knetsch, V. Libov *et al.*, "Tunable plasma-based energy dechirper," *Phys. Rev. Lett.* **122**, 034801 (2019).
- ¹⁰V. Shpakov, M. P. Anania, M. Bellaveglia, A. Biagioni, F. Bisesto, F. Cardelli, M. Cesarini, E. Chiadroni, A. Cianchi, G. Costa *et al.*, "Longitudinal phase-space manipulation with beam-driven plasma wakefields," *Phys. Rev. Lett.* **122**, 114801 (2019).
- ¹¹V. P. Drachev, Y. I. Krasnikov, and P. A. Bagryansky, "Dispersion interferometer for controlled fusion devices," *Rev. Sci. Instrum.* **64**, 1010–1013 (1993).
- ¹²E. Stambulchik, S. Alexiou, H. R. Griem, and P. C. Keppel, "Stark broadening of high principal quantum number hydrogen balmer lines in low-density laboratory plasmas," *Phys. Rev. E* **75**, 016401 (2007).
- ¹³J. M. Palomares, S. Hübner, E. A. D. Carbone, N. De Vries, E. M. Van Veldhuizen, A. Sola, A. Gamero, and J. J. A. M. Van Der Mullen, " H_{β} Stark broadening in cold plasmas with low electron densities calibrated with Thomson scattering," *Spectrochim. Acta, Part B* **73**, 39–47 (2012).
- ¹⁴F. Mackel, P. Kempkes, J. Tenfelde, S. Ridder, and H. Soltwisch, "Triple probe measurements benchmarked by interferometry in a pulsed-power plasma," *Contrib. Plasma Phys.* **53**, 33–38 (2013).
- ¹⁵F. Filippi, M. Anania, A. Biagioni, E. Chiadroni, A. Cianchi, M. Ferrario, A. Gribono, A. Mostacci, L. Palumbo, and A. Zigler, "Plasma density profile characterization for resonant plasma wakefield acceleration experiment at SPARC_LAB," in

- 7th International Particle Accelerator Conference (IPAC'16), Busan, Korea, 8–13 May 2016, <http://www.jacow.org>, pp. 2554–2556.
- ¹⁶F. Filippi, M. P. Anania, A. Biagioni, E. Chiadroni, A. Cianchi, M. Ferrario, A. Mostacci, L. Palumbo, and A. Zigler, “Spectroscopic measurements of plasma emission light for plasma-based acceleration experiments,” *J. Instrum.* **11**, C09015 (2016).
- ¹⁷J. Van Tilborg, A. J. Gonsalves, E. H. Esarey, C. B. Schroeder, and W. P. Leemans, “Density characterization of discharged gas-filled capillaries through common-path two-color spectral-domain interferometry,” *Opt. Lett.* **43**, 2776–2779 (2018).
- ¹⁸J. Van Tilborg, A. J. Gonsalves, E. Esarey, C. B. Schroeder, and W. P. Leemans, “High-sensitivity plasma density retrieval in a common-path second-harmonic interferometer through simultaneous group and phase velocity measurement,” *Phys. Plasmas* **26**, 023106 (2019).
- ¹⁹R. Roussel, G. Andonian, J. Rosenzweig, and S. Baturin, “Longitudinal current profile reconstruction from wakefield response in plasmas and structures,” *Phys. Rev. Accelerators and Beams* **23**(12), 121303 (2020).
- ²⁰G. Loisch, G. Asova, P. Boonpornprasert, Y. Chen, J. Good, M. Gross, H. Huck, D. Kalantaryan, M. Krasilnikov, O. Lishilin *et al.*, “Plasma density measurement by means of self-modulation of long electron bunches,” *Plasma Phys. Controlled Fusion* **61**, 045012 (2019).
- ²¹P. Chen, J. M. Dawson, R. W. Huff, and T. Katsouleas, “Acceleration of electrons by the interaction of a bunched electron beam with a plasma,” *Phys. Rev. Lett.* **54**, 693 (1985).
- ²²T. Katsouleas, S. Wilks, P. Chen, J. Dawson, and J. Su, “Beam loading in plasma accelerators,” *Part. Accel.* **22**, 81–99 (1987); available at https://accelconf.web.cern.ch/p87/PDF/PAC1987_0100.PDF
- ²³W. Lu, C. Huang, M. Zhou, W. Mori, and T. Katsouleas, “Limits of linear plasma wakefield theory for electron or positron beams,” *Phys. Plasmas* **12**, 063101 (2005).
- ²⁴M. Ferrario *et al.*, “SPARC_LAB present and future,” *Nucl. Instrum. Methods Phys. Res., Sect. B* **309**, 183–188 (2013).
- ²⁵E. Chiadroni *et al.*, “The SPARC linear accelerator based terahertz source,” *Appl. Phys. Lett.* **102**, 094101 (2013).
- ²⁶P. A. Walker, P. Alesini, A. Alexandrova, M. P. Anania, N. Andreev, I. Andriyash, A. Aschikhin, R. Assmann, T. Audet, A. Bacci *et al.*, “Horizon 2020 EuPRAXIA design study,” *J. Phys.: Conf. Ser.* **874**, 012029 (2017).
- ²⁷M. Ferrario, D. Alesini, M. Anania, M. Artioli, A. Bacci, S. Bartocci, R. Bedogni, M. Bellaveglia, A. Biagioni, F. Bisesto *et al.*, “EuPRAXIA@SPARC_LAB design study towards a compact FEL facility at LNF,” *Nucl. Instrum. Methods Phys. Res., Sect. A* **909**, 134–138 (2018).
- ²⁸M. Weikum, T. Akhter, P. Alesini, A. Alexandrova, M. Anania, N. Andreev, I. Andriyash, A. Aschikhin, R. Assmann, T. Audet *et al.*, “EuPRAXIA—A compact, cost-efficient particle and radiation source,” *AIP Conf. Proc.* **2160**, 040012 (2019).
- ²⁹D. Alesini, G. Di Pirro, L. Ficcadenti, A. Mostacci, L. Palumbo, J. Rosenzweig, and C. Vaccarezza, “RF deflector design and measurements for the longitudinal and transverse phase space characterization at SPARC,” *Nucl. Instrum. Methods Phys. Res., Sect. A* **568**, 488–502 (2006).
- ³⁰A. Cianchi, D. Alesini, M. Anania, A. Bacci, M. Bellaveglia, M. Castellano, E. Chiadroni, D. Di Giovenale, G. Di Pirro, M. Ferrario *et al.*, “Six-dimensional measurements of trains of high brightness electron bunches,” *Phys. Rev. Spec. Top.—Accel. Beams* **18**, 082804 (2015).
- ³¹N. Barov, J. Rosenzweig, M. Thompson, and R. Yoder, “Energy loss of a high-charge bunched electron beam in plasma: Analysis,” *Phys. Rev. Spec. Top.—Accel. Beams* **7**, 061301 (2004).
- ³²S. Romeo, “Beam loading assisted matching working point for PWFA beam driven experiment at SPARC_LAB,” Ph.D. thesis, La Sapienza, University of Rome, 2017.
- ³³A. Marocchino, F. Massimo, A. Rossi, E. Chiadroni, and M. Ferrario, “Efficient modeling of plasma wakefield acceleration in quasi-non-linear-regimes with the hybrid code architect,” *Nucl. Instrum. Methods Phys. Res., Sect. A* **829**, 386 (2016).
- ³⁴H. Wiedemann, *Particle Accelerator Physics* (Springer, 2015).
- ³⁵W. Lu, C. Huang, M. Zhou, M. Tzoufras, F. Tsung, W. Mori, and T. Katsouleas, “A nonlinear theory for multidimensional relativistic plasma wave wakefields,” *Phys. Plasmas* **13**, 056709 (2006).